

# Analysis of a Resonant Reset Condition for a Single-Ended Forward Converter

Naoki MURAKAMI and Mikio YAMASAKI

NTT Applied Electronics Laboratories  
3-9-11, Midori-cho, Musashino-shi, Tokyo, 180 Japan

## ABSTRACT

The reset condition of a transformer core flux is analyzed for a single-ended forward converter operating in a resonant reset mode. Relationships between reset time and device parameters such as a main switch output capacitance are derived. As a result, the maximum frequency in a resonant reset mode can be predicted.

## INTRODUCTION

In a single-ended forward converter, it is necessary to reset transformer core flux during main switch off time to prevent transformer core saturation. To avoid core saturation and to limit the peak voltage across the main switch, additional reset windings and reset circuits are widely used in forward converters [1], [2]. At a higher switching frequency, such as 500 kHz, converters can operate without these mechanisms because core flux is reset by the resonance of transformer magnetizing inductance and parasitic capacitances of switching devices [3],[4]. This is called the "resonant reset mode".

Elimination of the reset mechanism eliminates power loss in the reset circuit, thus simplifying circuitry and increasing efficiency. However, transformer flyback voltage and reset time are strongly affected by device parameters such as main switch output capacitance.

In this paper, relationships between these device parameters and transformer reset time are analyzed, and reset time necessary to prevent core flux saturation is derived.

## OPERATION STATES AND MODES

The basic circuit configuration of a single-ended forward converter is shown in Fig.1. The transformer  $T_m$  is reset by oscillation caused by transformer magnetizing inductance  $L_m$ , main switch output capacitance  $C_Q$  and diode junction capacitance  $C_{D1}$ .

Possible operation states of main switch  $Q$ , and diodes  $D_1$  and  $D_2$ , are listed in

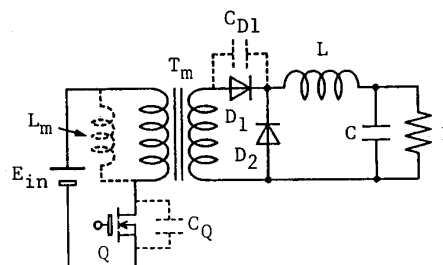


Fig. 1 Single-ended forward converter without reset mechanism.

Table 1 Operation states for the circuit shown in Fig. 1.

	Q	D <sub>1</sub>	D <sub>2</sub>
State A	ON	ON	ON
State B		ON	OFF
State C		OFF	ON
State D		OFF	OFF
State E	OFF	ON	ON
State F		ON	OFF
State G		OFF	ON
State H		OFF	OFF

Table 1. "ON" indicates that the main switch forward current path has a low resistance or that the diode is forward-biased. Conversely, "OFF" indicates that the main switch forward current path has a high resistance or that the diode is reverse-biased. States A, B and F occur during main switch turn-on, on-state and turn-off. State E occurs during main switch turn-off or after flyback transformer voltage falls to zero. State G occurs during resonant reset. States D and H don't occur while the smoothing inductor current flows continuously, because either diode  $D_1$  or diode  $D_2$  must be in the on-state. In practice, the converter operates in this condition. Therefore, the analysis focuses on the continuous current mode of the smoothing inductor. State transition occurs when one element turns on or off. The state transition flow diagram is shown in Fig. 2.

Possible resonant reset modes and their sequences are obtained from Fig. 2 and shown in Table 2. Each mode comprises five operation states. Mode 1 occurs when the main switch turns on after the transformer flyback voltage falls to zero. Mode 2 occurs when the main switch turns on while the flyback voltage is being induced in the transformer. The main switch voltage applied just before the main switch turns on is higher in this mode than that in Mode 1. This voltage determines main switch power loss caused by parasitic capacitances of the main switch[5]. Mode 1 is preferred for higher efficiency and is analyzed as follows.

### ANALYSIS

In this section, the exact analytical expressions are obtained which describe the converter currents and voltages in Mode 1.

### Nomenclature

Definition of symbols used here are as follows:

$T_1$ - $T_5$ :time during which the state transition occurs.  
 $T$ :switching period.  
 $t$ :time.  
 $L_{L1}$ :transformer primary leakage inductance.  
 $L_{L2}$ :transformer secondary leakage inductance\*.  
 $L_m$ :transformer magnetizing inductance.  
 $C_Q$ :main switch output capacitance.  
 $C_{D1}$ :forward diode junction capacitance\*.  
 $C_{D2}$ :freewheel diode junction capacitance\*.  
 $I_o$ :DC output current\*.  
 $E_{in}$ :DC input voltage.  
 $V_Q$ :main switch voltage.  
 $V_{D1}$ :forward diode reverse voltage\*.  
 $V_{D2}$ :freewheel diode reverse voltage\*.  
 $V_T$ :transformer primary voltage.  
 $i_Q$ :main switch current.  
 $i_2$ :transformer secondary current\*.  
 $i_m$ :transformer magnetizing current.  
 $i_{D1}$ :forward diode current\*.  
 $i_{D2}$ :freewheel diode current\*.

(\*) indicates values reflected from the primary winding of the main transformer.

### Assumptions

The following assumptions are made:

- (1) Transformer leakage inductances are considerably smaller than magnetizing inductance, that is  $L_{L1}, L_{L2} \ll L_m$ . Transformer winding resistances, stray capacitances and core loss are negligible. The transformer equivalent circuit is as shown in Fig. 3.
- (2) Main switch  $Q$ , and diodes  $D_1$  and  $D_2$  behave as short-circuits in the on-state and capacitors ( $C_Q, C_{D1}$  and  $C_{D2}$  respectively)

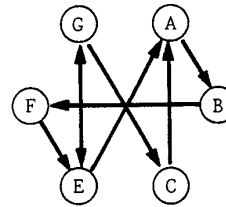


Fig. 2 State transition flow of a resonant reset mode.

Table 2 Operation modes for the circuit shown in Fig. 1.

	Sequence of states
Mode 1	$A \rightarrow B \rightarrow F \rightarrow E \rightarrow G \rightarrow A$
Mode 2	$A \rightarrow B \rightarrow F \rightarrow E \rightarrow G \rightarrow C \rightarrow A$

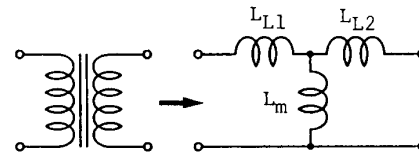


Fig. 3 Equivalent circuit for a main transformer.

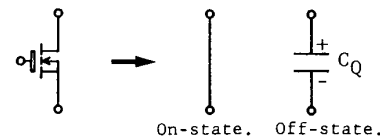


Fig. 4 Equivalent circuit for a main switch.

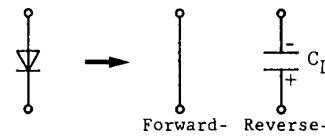


Fig. 5 Equivalent circuit for a diode.

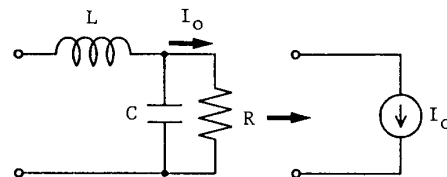


Fig. 6 Equivalent circuit for an output smoothing filter.

in the off-state. Diode recovery time is negligible. The equivalent circuits are as shown in Figs. 4 and 5.

(3) Output smoothing inductance  $L$  is large enough to consider output current constant. The equivalent circuit is as shown in Fig. 6.

(4) Current through inductance  $L$  is continuous.

### Analytical expressions

Based on these assumptions, the equivalent circuits for States A - G are as shown in Fig. 7.

Analysis is started for State A. Before time  $t=0$ , the forward converter is operating in State E as shown in Table 2. In this state, Q is in off-state, and  $D_1$  and  $D_2$  are in on-state.

#### Interval $T_1$ (State A) $0 < t < T_1$

At  $t=0$ , Q turns on, and State A begins. The operating equations derived from Fig. 7 are :

$$i_2 = (E_{in}/L_L)t + i_2(0) \quad (1)$$

$$i_m = [L_{L2}/(L_L L_m)] E_{in} t + i_m(0) \quad (2)$$

$$v_Q = v_{D1} = v_{D2} = 0 \quad (3)$$

where

$i_2(0)$  and  $i_m(0)$  are initial values.

$$L_L = L_{L1} + L_{L2} \quad (4)$$

At  $t=T_1$ ,  $i_2$  reaches  $I_o$  and  $D_2$  turns off. Operation then changes from State A to State B.

$T_1$  is given by:

$$T_1 = L_L(I_o - i_2(0))/E_{in} \quad (5)$$

#### Interval $T_2 - T_1$ (State B) $T_1 < t < T_2$

During this interval, energy is transferred from  $E_{in}$  to the load.

The operating equations are:

$$i_2 = I_o + E_{in} \sqrt{C_{D2}/L_L} \sin(W_B(t - T_1)) \quad (6)$$

$$i_m = (E_{in}/L_m)(t - T_1) + i_m(0) \quad (7)$$

$$+ E_{in}(L_{L1}/L_m) \sqrt{C_{D2}/L_L} \sin(W_B(t - T_1)) \quad (7)$$

$$v_{D2} = E_{in}[1 - \cos(W_B(t - T_1))] \quad (8)$$

$$v_Q = v_{D1} = 0 \quad (9)$$

where

$$W_B = 1/\sqrt{L_L C_{D2}} \quad (10)$$

$$i_m(T_1) = \frac{L_{L2}}{L_L} \frac{E_{in} T_1}{L_m} + i_m(0) \quad (11)$$

An oscillation caused by  $L_{L1}$ ,  $L_{L2}$  and  $C_{D2}$  reduces with time due to the resistances of main switch, diodes and windings (neglected in this analysis). Therefore, the second terms of equations (6)-(8) eventually reach zero.

This interval ends at  $T_2$  when the main switch turns off.

#### Interval $T_3 - T_2$ (State F) $T_2 < t < T_3$

During this interval,  $C_Q$  is charged and  $C_{D2}$  is discharged.

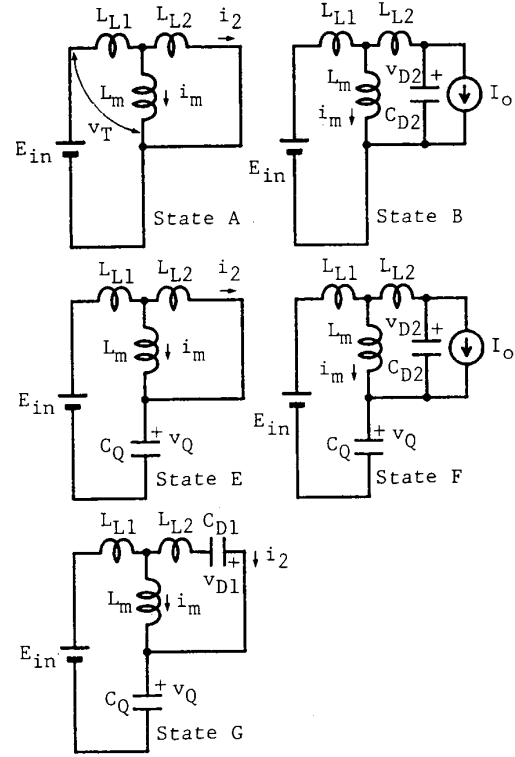


Fig. 7 Equivalent circuit for a resonant reset mode.

The operating equations are:

$$i_2 = I_o - \frac{C_{D2}}{C_Q + C_{D2}} X_F \sin(W_F(t - T_2) + Y_F) \quad (12)$$

$$i_m = X_F \sin(W_F(t - T_2) + Y_F) - I_o \quad (13)$$

$$v_{D2} = Z_F X_F \cos(W_F(t - T_2) + Y_F) \quad (14)$$

$$v_Q = E_{in} - v_{D2} \quad (15)$$

$$v_{D1} = 0 \quad (16)$$

where

$$i_m(T_2) = (E_{in}/L_m)(T_2 - T_1) + i_m(T_1) \quad (17)$$

$$W_F = 1/\sqrt{L_m(C_Q + C_{D2})} \quad (18)$$

$$X_F = \sqrt{(E_{in}/Z_F)^2 + (I_o + i_m(T_2))^2} \quad (19)$$

$$Y_F = \arctan[Z_F(I_o + i_m(T_2))/E_{in}] \quad (20)$$

$$Z_F = \sqrt{L_m/(C_Q + C_{D2})} \quad (21)$$

This interval ends at  $t=T_3$  when  $v_{D2}$  reaches zero, and  $C_{D2}$  is entirely discharged.

$$T_3 = (\pi/2 - Y_F)/W_F + T_2 \quad (22)$$

#### Interval $T_4 - T_3$ (State E) $T_3 < t < T_4$

At  $t=T_3$ , diode  $D_2$  turns on, and State E

begins. During this interval,  $C_Q$  is charged by the remaining energy stored in  $L_{L1}$  and  $L_{L2}$ . This interval is very short, so we assume for simplicity that the magnetizing current is constant.

The operating equations are:

$$i_2 = (i_2(T_3) + i_m(T_3)) \cos(\omega_E(t - T_3)) - i_m(T_3) \quad (23)$$

$$i_m = i_m(T_3) \quad (24)$$

$$v_Q = E_{in} + Z_E(i_2(T_3) + i_m(T_3)) \sin(\omega_E(t - T_3)) \quad (25)$$

$$v_{D1} = v_{D2} = 0 \quad (26)$$

$$\text{where} \quad i_2(T_3) = I_o - \frac{C_{D2}}{C_Q + C_{D2}} X_F \quad (27)$$

$$i_m(T_3) = X_F - I_o \quad (28)$$

$$\omega_E = 1 / \sqrt{L_L C_Q} \quad (29)$$

$$Z_E = \sqrt{L_L / C_Q} \quad (30)$$

This interval ends at  $t = T_4$  when  $i_2$  reaches zero, i.e. the energy stored in  $L_{L1}$  and  $L_{L2}$  is transferred to  $C_Q$ .

$$T_4 = \frac{1}{\omega_E} \arccos\left(\frac{i_m(T_3)}{i_2(T_3) + i_m(T_3)}\right) + T_3 \quad (31)$$

**Interval T5-T4** (State G)  $T_4 < t < T_5$

At  $t = T_4$ ,  $D_1$  turns off and an oscillation caused by  $L_m$ ,  $C_Q$  and  $C_{D1}$  occurs.

The operating equations are:

$$i_2 = - \frac{C_{D1}}{C_Q + C_{D1}} i_m \quad (32)$$

$$i_m = X_G \cos(\omega_G(t - T_4) + Y_G) \quad (33)$$

$$v_Q = E_{in} + X_G Z_G \sin(\omega_G(t - T_4) + Y_G) \quad (34)$$

$$v_{D1} = v_Q - E_{in} \quad (35)$$

$$v_{D2} = 0 \quad (36)$$

$$\text{where} \quad \omega_G = 1 / \sqrt{L_m (C_Q + C_{D1})} \quad (37)$$

$$X_G = \sqrt{i_m^2(T_4) + (v_Q(T_4) - E_{in})^2 / Z_G^2} \quad (38)$$

$$Y_G = \begin{cases} \arctan\left(\frac{v_Q(T_4) - E_{in}}{Z_G i_m(T_4)}\right) & i_m(T_4) > 0 \\ \pi - \arctan\left(\frac{v_Q(T_4) - E_{in}}{-Z_G i_m(T_4)}\right) & i_m(T_4) < 0 \end{cases} \quad (39)$$

$$\pi - \arctan\left(\frac{v_Q(T_4) - E_{in}}{-Z_G i_m(T_4)}\right) \quad i_m(T_4) < 0 \quad (40)$$

$$Z_G = \sqrt{L_m / (C_Q + C_{D1})} \quad (41)$$

$$i_m(T_4) = i_m(T_3) \quad (41)$$

$$v_Q(T_4) = E_{in} \quad (42)$$

$$+ Z_E \sqrt{\left(\frac{C_Q}{C_Q + C_{D2}}\right) (I_o + i_m(T_3))^2 - i_m(T_3)^2} \quad (42)$$

This interval ends at  $t = T_5$  when  $v_{D1}$  reaches zero, that is, when transformer

flyback voltage reaches zero.

$$T_5 = (\pi - Y_G) / \omega_G + T_4 \quad (43)$$

**Interval T-T5** (State E)  $T_5 < t < T$

At  $t = T_5$ ,  $D_1$  turns on again, and the operation state changes to State E.

During this interval, the secondary transformer winding is shorted by  $D_1$  and  $D_2$ .  $i_m$  flows through  $D_1$  and  $D_2$  and remains constant until  $Q$  turns on. Ignoring the oscillation caused by  $L_{L1}$ ,  $L_{L2}$  and  $C_Q$  at the beginning of this state.

The operating equations are:

$$i_2 = i_2(T_5) = \frac{C_{D1}}{C_Q + C_{D1}} X_G \quad (44)$$

$$i_m = i_m(T_5) = -X_G \quad (45)$$

$$v_Q = v_{D1} = v_{D2} = 0 \quad (46)$$

In a steady state, final values of equations (44)-(46) become the initial values of State A.  $i_m(0)$  and  $i_2(0)$  are derived from equations (5), (11), (17), (28), (41)-(45) as follows:

$$i_m(0) = - \frac{A}{2I_m} - \frac{C_Q + C_{D1}}{C_Q} \frac{B}{2A} \quad (47)$$

$$i_2(0) = -[C_{D1} / (C_Q + C_{D1})] i_m(0) \quad (48)$$

where

$$A = E_{in} T_2 - L_{L1} I_o \quad (49)$$

$$B = [C_Q / (C_Q + C_{D2})]^2 (L_{L1} + L_{L2}) I_o^2 \quad (50)$$

$i_m(T_2)$  is derived from equations (11), (17) and (47).

$$i_m(T_2) = \frac{A}{2I_m} - \frac{C_Q + C_{D1}}{C_Q} \frac{B}{2A} \quad (51)$$

Using these expressions, voltage and current waveforms can be illustrated as shown in Figs. 8 and 9. The waveforms in Fig. 8 are observed in a normal condition and those in Fig. 9 are observed where the main switch on-time is very short, load current is large and overcurrent protection is working.

The magnetizing current dependence on output current is shown in Fig. 10. Parameter values used for the calculation are:

$$L_m = 0.74 \text{ mH}, L_{L1} = L_{L2} = 0.18 \text{ } \mu\text{H}, T = 5 \text{ } \mu\text{s}$$

$$C_Q = 220 \text{ pF}, C_{D1} = C_{D2} = 11 \text{ pF}, E_{in} = 50 \text{ v.}$$

In Fig. 10, the areas where  $i_m$  is above zero and below zero correspond to the first and third quadrants of the B-H plane, respectively. It is clear that main transformer core flux excursions between the first and third quadrant in B-H characteristics. This is similar to a push-pull converter. The flux excursion is almost symmetrical at a light load. As the load becomes heavy, the center of flux excursion moves into the third quadrant.

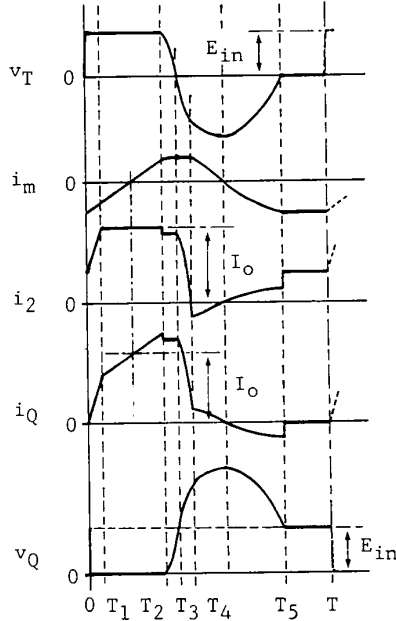


Fig. 8 Current and voltage waveforms for  $i_m(T_4) > 0$ .

When a load is heavy and main switch on-time is very short, the flux excursion is entirely in the third quadrant.

#### RESET CONDITION

To reduce power loss of main switch, parameters should be fixed so that flyback voltage falls to zero before a new cycle is commenced. From the above equations, the following condition must be satisfied.

$$T_5 = (\pi - Y_G) / W_G + T_2 < T \quad (52)$$

In the worst case, where  $I_0$  is very small, this equation is simplified as follows:

$$T_5 = \pi / W_G + T_2 < T \quad (53)$$

Maximum frequency ( $F_{max}$ ) operating at a resonant reset mode is determined from this equation as follows:

$$F_{max} = (1-D) / (\pi \sqrt{L_m(C_Q + C_{D1})}) \quad (54)$$

where

$D = T_2 / T$  : main switch duty ratio.

The maximum frequency dependence on  $C_Q$  and  $C_{D1}$  is shown in Fig. 11.

Furthermore, maximum flyback voltage of the main transformer ( $V_m$ ) under main switch breakdown voltage ( $V_{QM}$ ) or diode reverse voltage ( $V_{DR}$ ) must be limited.

From equation (34),

$$V_m = X_G Z_G < V_{QM} - E_{in} \text{ or } V_{DR} \quad (55)$$

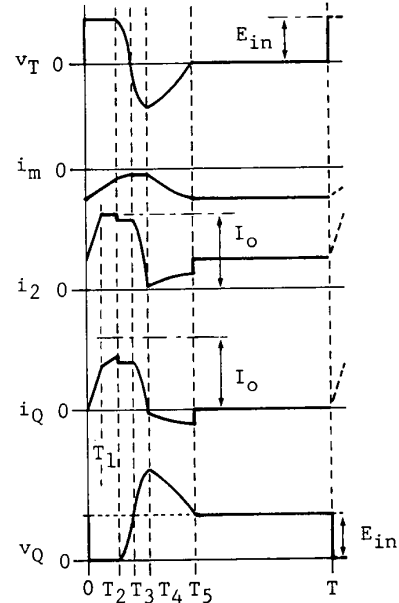


Fig. 9 Current and voltage waveforms for  $i_m(T_4) < 0$ .

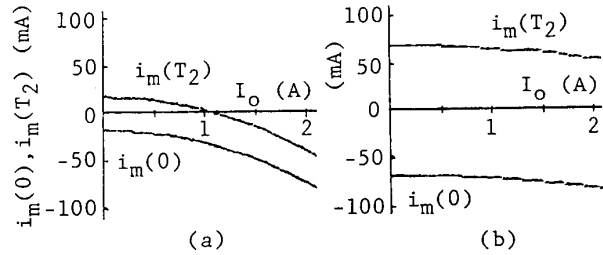


Fig. 10 Magnetizing current dependence on output current. (a)  $T_2 = 0.5 \mu s$ , (b)  $T_2 = 2 \mu s$ . ( $D = 0.1$ ) ( $D = 0.4$ )

Thus,

$$\sqrt{\frac{W_G^2}{4} \left( A - \frac{B}{C_Q W_G^2 A} \right)^2 + \frac{B}{C_Q}} < V_{QM} - E_{in} \text{ or } V_{DR} \quad (56)$$

The flyback voltage dependences on main switch output capacitance are shown in Fig. 12. The parameters used here are the same as those used in the previous section.

In this converter design, the parameters must satisfy equations (54) and (56).

#### EXPERIMENTAL RESULTS

To confirm the validity of the analysis presented above, analytical and experimental results are compared. A low power DC-to-DC converter with a 50 volt input and a 5 volt, 2 amperes maximum output is employed for the experiments, since the effect of transformer magnetizing current is emphasized.

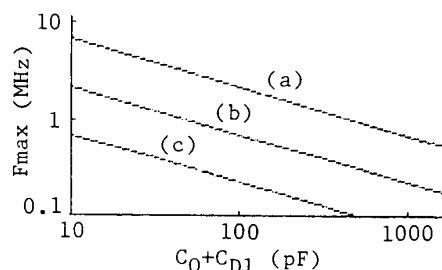


Fig. 11 Maximum frequency dependence on  $C_Q$  and  $C_{D1}$  at  $D=0.4$ .  
(a)  $L_m=0.074$  mH. (b)  $L_m=0.74$  mH.  
(c)  $L_m=7.4$  mH.

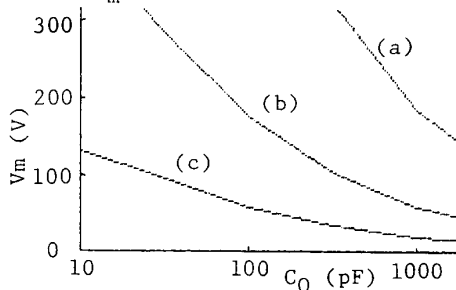


Fig. 12 Maximum flyback voltage dependence on  $C_Q$  at  $D=0.4$ ,  $I_O=0.5$  A.  
(a)  $L_m=0.074$  mH,  $L_{L1}=L_{L2}=0.018$   $\mu$ H.  
(b)  $L_m=0.74$  mH,  $L_{L1}=L_{L2}=0.18$   $\mu$ H.  
(c)  $L_m=7.4$  mH,  $L_{L1}=L_{L2}=1.8$   $\mu$ H.

Experimental and analytical converter voltages and current waveforms are compared in Fig. 13. The analytical parameters are the same as the previous ones. There is good correlation between them. The small differences observed when the main switch turns off are due to the assumption that main switch output capacitance and diode junction capacitance are constant.

### CONCLUSION

Transformer reset condition is derived for a single-ended forward converter operating at a resonant reset mode. Main results obtained from the analysis are:  
(1) The resonance period of the main transformer flyback voltage is mainly determined by transformer magnetizing inductance, main switch output capacitance and diode junction capacitance.  
(2) The main transformer flux excursion is between the first and third quadrant in B-H characteristics. With a light load, it is almost symmetrical. With a heavy load and very short main switch on-time on the other hand, it is entirely in the third quadrant.  
(3) Maximum frequency operating in the resonant reset mode is determined by the above parameters and volt-second products during main switch on-time.

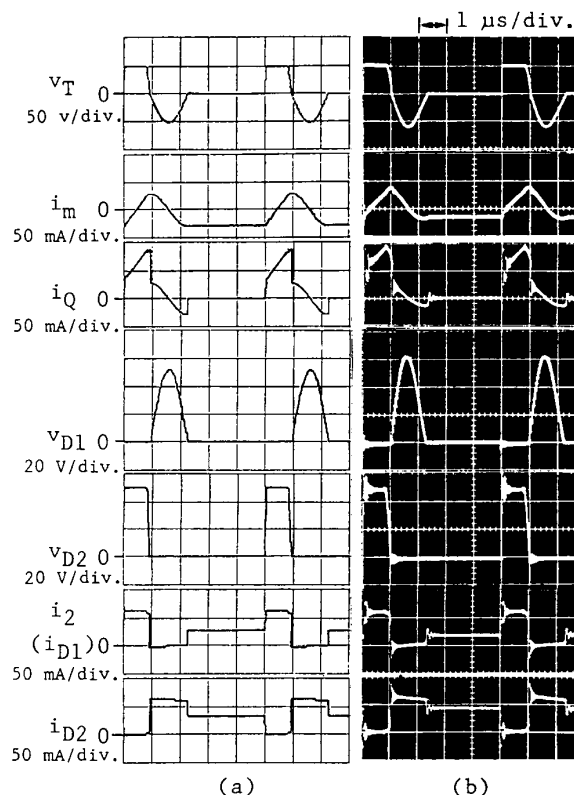


Fig.13 Comparison of calculated and measured waveforms at  $T_2=0.8$   $\mu$ s ( $D=0.16$ ),  $I_O=62.5$  mA (0.5 W output).  
(a) Calculated. (b) Measured.

### ACKNOWLEDGMENTS

The authors would like to thank Katsuichi Yotsumoto and Kunio Moriya for their helpful comments.

### REFERENCES

- [1] R. P. Severns and G. Bloom, Modern DC-TO-DC Switchmode Power Converter Circuits, New York, Van Nostrand Reinhold, 1984, pp. 130-135.
- [2] Y. Fukuhara and K. Tsukamoto, "Power Pack Technology for NTT Digital Local Switching System", INTELEC '83 Rec., pp. 247-248, 1983.
- [3] K. Yamamoto and Y. Aoyama, "1 MHz Self Reset Type Single-Ended Forward Converter (in Japanese)", Nat. Conv., IECE of Japan, No. 648, March, 1984.
- [4] K. Wallace, "Resonant Reset", IBM Technical Disclosure Bulletin, Vol. 26, No. 11, pp. 6179-6180, April, 1984.
- [5] M. Chi and C. Hu, "An Intrinsic Power MOSFET Model for Circuit Design and Analysis", Powercon 10, PP. H-2, 1-9, 1983.